JOURNAL OF GEOPHYSICAL RESEARCH, VOL. 106, NO. B1, PAGES 703–712, JANUARY 10, 2001

Role of ocean-continent contrast and continental keels on plate motion, net rotation of lithosphere, and the geoid

Shijie Zhong[1]

Department of Earth, Atmospheric and Planetary Sciences, Massachusetts Institute of Technology, Cambridge

Abstract. Three-dimensional spherical shell models of mantle convection have been formulated to investigate the effects of ocean-continent contrast (i.e., different viscosity for continental and oceanic lithospheres) and continental keels on plate motion, net rotation of lithosphere (i.e., degree 1 toroidal plate motion), and the geoid. The models include relatively realistic plate rheology (i.e., strong plate interiors and weak plate margins) and continental keel structure based on seismic models. The mantle flow in the models is driven by slab buoyancy. The models demonstrate that the ocean-continent contrast and continental keels have minor effects on the long-wavelength geoid (for degrees 2-5). However, continental keels overriding subducted slabs, for example in North America, can produce large negative gravity anomalies at a regional scale. This may have important implications to interpreting the gravity anomalies in North America. Our models show that when plates bounded by weak plate margins have the same thickness, neither weak plate margins nor the ocean-continent contrast efficiently excite net rotation of lithosphere, although they excite toroidal motion at higher harmonic degrees. However, plate thickness variations like continental keels excite the net rotation. In spite of their ability to excite the net rotation, continental keels as thick as 300 km cannot provide the necessary coupling to the deep mantle to produce the observed net rotation of lithosphere and slow continental motion if there is a weak asthenosphere underlying them. If the thermomechanic structure of North American continental upper mantle derived from seismic and heat flow studies is representative, our models suggest that the temperature- and pressure-dependent mantle rheology may not produce sufficiently high viscosity below continental keels that is needed to explain the observed plate motion. Our study hints the necessity to include more realistic treatment of plate boundaries in future studies to assess possible effects of plate-plate coupling on plate motion.

1. Introduction

The geoid and the surface plate motion are the principal observations that pose the most direct constraints on the dynamic processes in the Earth's mantle [*Hager and Richards*, 1989; *Ricard et al.*, 1993; *Lithgow-Bertelloni and Richards*, 1998]. Plate motion is often described in a hot spot reference frame. This is because relative motion between hot spots in different oceans is much smaller than relative motion between plates [*Duncan*, 1981; *Morgan*, 1983; *Molnar and Stock*, 1987]. Important features of plate motion in a hot spot reference frame include (1) piecewise constant angular velocity for each plate; (2) faster motion for oceanic plates than continental plates [e.g., *Gordon and Jurdy*, 1986]. Spectral analyses show that the plate motion has toroidal components (i.e., representing plate motion associated with transform faults and oblique subduction) that are as large as its poloidal components (i.e., representing creation and subduction of sea-floor) for all wavelengths including degree 1 [*Hager and O'Connell*, 1978]. The toroidal motion at degree 1 represents a net rotation of Earth's surface with respect to the hot spot reference frame. The net rotation ranges from 0.2 to 0.45 rad/100 Ma, depending on plate motion models [*Gordon and Jurdy*, 1986; *Minster and Jordan*, 1978]. The net rotation results from the combination of large surface area and large motion for oceanic plates (mainly the Pacific plate) [*Ricard et al.*, 1991].

Plate motion is surface manifestation of mantle dynamics. Plate motion is not only sensitive to the distribution of mantle buoyancy, it also depends greatly on mechanical structure of lithosphere [*Gurnis*, 1989; *King and Hager*, 1990]. Particularly, weak plate margins that represent the most important lateral variations in mechanical structure are the source of toroidal components of plate motion [*Bercovici*, 1995; *Zhong and Gurnis*, 1996]. However, global dynamic models with either a torque balance [*Ricard et al.*, 1993; *Lithgow-Bertelloni and Richards*, 1998] or weak zone plate formulation [*Zhong and Davies*, 1999] often overestimate continental motions and predict them to be comparable with oceanic plate motions, although oceanic plate motions are reasonably reproduced. Because the difference between oceanic and continental plate motions contributes greatly to the net rotation, these models have difficulties in reproducing the net rotation of lithosphere. It has long been recognized that the net rotation has important implications to the physical significance of the hot spot reference frame [*Ricard et al.*, 1991; *O'Connell et al.*, 1991; *Forte and Peltier*, 1994].

[1]Now at Department of Physics, University of Colorado, Boulder, Colorado.

Paper number 2000JB900364.
0148-0227/01/2000JB900364$09.00

Therefore it is important to understand the dynamic origin of the large difference between oceanic and continental plate motions and the net rotation of lithosphere.

Differences in thermal, chemical, and mechanical structure between oceanic and continental plates that may cause a stronger coupling of continents to their underlying mantle (e.g., via continental keels) may be responsible for the difference between continental and oceanic plate motions and the lithospheric net rotation [*Ricard et al.*, 1991; *O'Connell et al.*, 1991]. Alternatively, the observed faster oceanic plate motions may result from asymmetric subduction with subducted slabs that as the main driving forces for convection are mainly coupled to oceanic plates [e.g., *Forsyth and Uyeda*, 1975]. Lateral variations in viscosity in the lower mantle may also introduce net rotation between the mantle and lithosphere [*Forte and Peltier*, 1994]. However, lateral variations in viscosity in the lower mantle may be less important than those in the upper mantle in producing lithospheric net rotation because plates are directly coupled to the upper mantle. It has also been reported that models with continents that are stronger than oceanic plates can improve the fit to the long-wavelength components of plate motion, but net rotation of lithosphere cannot be reproduced [*Wen and Anderson*, 1997].

How tectonic plates couple to each other and to their underlying mantle is crucial to plate motion and lithospheric net rotation. However, an understanding of these physical processes has been hindered by our ability in modeling them. For example, in the models by *Ricard et al.* [1991], lateral variations in viscosity are all confined in a 100-km-thick shell that overrides a mantle with a spherically symmetric viscosity structure. Their models treat the top shell with a thin shell approximation, and this may be difficult to fully account for the coupling associated with continental keels. In fact, two-dimensional calculations show that the influence of continental keels on plate motion depends on many variables including how the buoyancy is distributed relative to the continents and that continental keels may not necessarily reduce the continental motion [*Gurnis and Torsvik*, 1994]. In the models by *Wen and Anderson* [1997], continental keels were not considered, and their relatively coarse resolution (l_{max}=12) may prevent plates from being decoupled from each other as effectively as they would.

The main purpose of this paper is to address how continental keels and the ocean-continent contrast influence plate motion including lithospheric net rotation by using global models with well-resolved weak plate margins and continental keels that are derived from seismic models (Figure 1a) [*Grand*, 1994]. We will also assess the effects of these continental structures on the geoid. Although significant progress has been made in modeling global mantle convection in the last decade [*Glatzmaier et al.*, 1990; *Bunge et al.*, 1996], answers to the above questions were not possible until recently. This is because of the difficulties in modeling large lateral variations in mantle viscosity at a high resolution. Global dynamic models with lateral variations in viscosity were previously developed with spectral [*Zhang and Christensen*, 1993], finite volume [*Ratcliff et al.*, 1996], and semianalytic methods [*Forte and Peltier*, 1994; *Wen and Anderson*, 1997]. Recent developments of a finite element code CitcomS based on parallel computing technology by *Zhong and Davies* [1999] and *Zhong et al.* [2000] have made it possible for such modeling at a reasonably high resolution. In what follows, we will first describe model specifications. Second, we will present results and analyses. The last sections are devoted to discussions and conclusions.

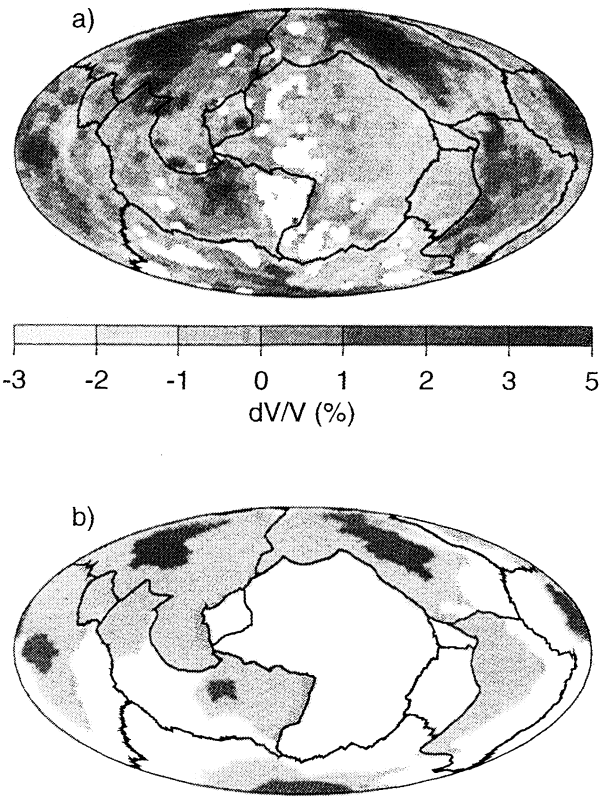

Figure 1. (a) *S* wave velocity anomalies in percentage at a depth of 250 km by *Grand* [1994]. The anomalies in the white areas are unspecified. Plate boundaries are also shown. (b) A schematic representation of lithospheric structure used in instantaneous flow models. The structure includes oceanic plates, continents, continental keels, and plate boundaries.

2. Model Description

The mantle flow is treated as an incompressible Stokes flow. The flow is driven by negative buoyancy of slabs whose spatial distribution has been predicted from the past 160 Myr of subduction history [*Ricard et al.*, 1993]. Buoyant upwellings are ignored because it has been inferred that mantle flow is caused predominantly by the cooling of the top thermal boundary layer (the lithosphere), with only ~10% of the mantle heat budget being transported by mantle plumes rising from a bottom thermal boundary layer (e.g., the core-mantle boundary) [*Davies*, 1988; *Sleep*, 1990]. An alternative way to estimate the buoyancy distribution is to convert seismic tomography structures into a density model. Recent high-resolution tomography models are dominated by slab-like structures beneath subduction zones [*van der Hilst et al.*, 1997; *Grand et al.*, 1997], and the slab density model shows broad similarities to the tomography models.

To focus on the effect of continents, our models include lateral variations in viscosity only in the upper mantle and lithosphere. Except for one model that will be discussed later, the nondimensional viscosities in the lower mantle, the transition zone, and the upper mantle (excluding the regions

Table 1. Model Parameters[a]

Case	D_{ck}, km	η_{lith_c}	R_u
1	100	300	1
2	100	3000	1
3	300	300	1
4	410	300	1
5	300	300	10

[a] D_{ck} is the depth of continental keels; η_{lith_c} is the viscosity for continents (100 km thick except in regions with the keels); and R_u is the ratio of viscosity increase from 200 to 410 km in the upper mantle. For all cases, the viscosities for the oceanic lithosphere (0-100 km), upper mantle (100-410 km), transition zone (410-670 km), and lower mantle (670-2900 km) are 300, 0.1, 3.0, and 30, respectively. Plate margin viscosity is 1.

occupied by continental keels) are 30, 3, and 0.1, respectively, consistent with previous studies [*Hager and Richards*, 1989] (Table 1). Lateral variations in lithospheric viscosity are prescribed according to the geometry of surface plates and continents (Figure 1b). Plate thickness is 100 km for both oceanic and continental plates, but continental keels may extend to a greater depth. Lithospheric viscosity structure to first order can be approximated with strong plate interiors that are surrounded by weak plate margins, and such a lithospheric viscosity structure is essential to reproduce a nearly constant angular velocity for each plate [*Zhong and Davies*, 1999]. The viscosities of plate margins and plates are set to be 1 and 300, respectively (Table 1). The plate margins are assumed to be 400 km wide regardless of their tectonic style.

The geometry of continental keels (Figure 1b) is taken from a *S* wave tomography model [*Grand*, 1994] in which seismically fast anomalies are clearly seen below old cratons such as the North American and Siberian cratons to a depth of >300 km (Figure 1a). Other *S* wave tomography models show similar seismic structures [e.g., *Woodhouse and Dziewonski*, 1984; *Ritzwoller and Lavely*, 1995; *Su et al.*, 1994; *Masters et al.*, 1996; *Li and Romanowicz*, 1996]. Since the depth extent of these anomalies is less well constrained, the thickness of continental keels is treated as a variable in the models. Continental keels may need to be significantly stiffer than the ambient mantle in order to survive over the geological history [*Shapiro et al.*, 1999; *Manga and O'Connell*, 1995]. Stiff continental lithosphere may result from de-volatilization as continental crust is formed [*Pollack*, 1986]. In the models, continental keels have the same viscosity as continents whose viscosity is the same as that for oceanic plates except in one case as will be discussed later.

The top and core-mantle boundaries are subjected to free slip boundary conditions. With these boundary conditions the momentum equation and continuity equation are solved with CitcomS to obtain velocity and dynamic topography at the bottom and top boundaries [*Zhong and Davies*, 1999; *Zhong*

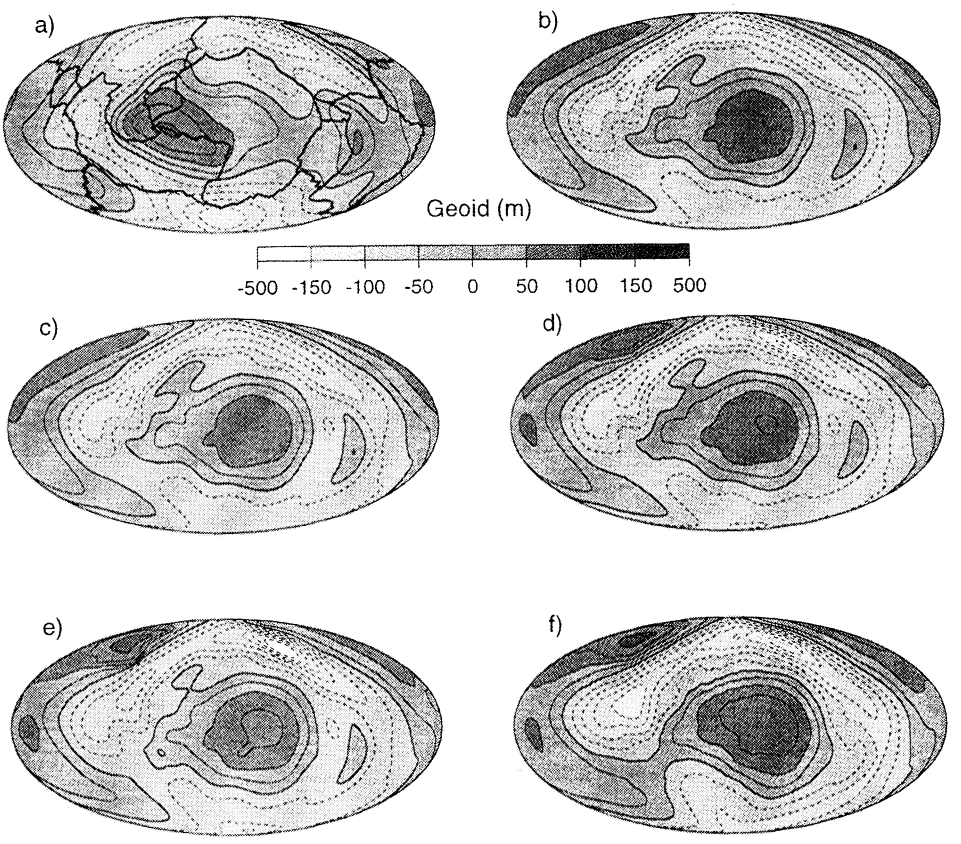

Figure 2. (a) The observed long-wavelength geoid (degrees 2 to 12) and model geoid from cases (b) 1, (c) 2, (d) 3, (e) 4, and (f) 5 with different mechanical structure for continents and the upper mantle. Heavy shadings and solid contours are for positive geoid anomalies. The contour interval is 25 m.

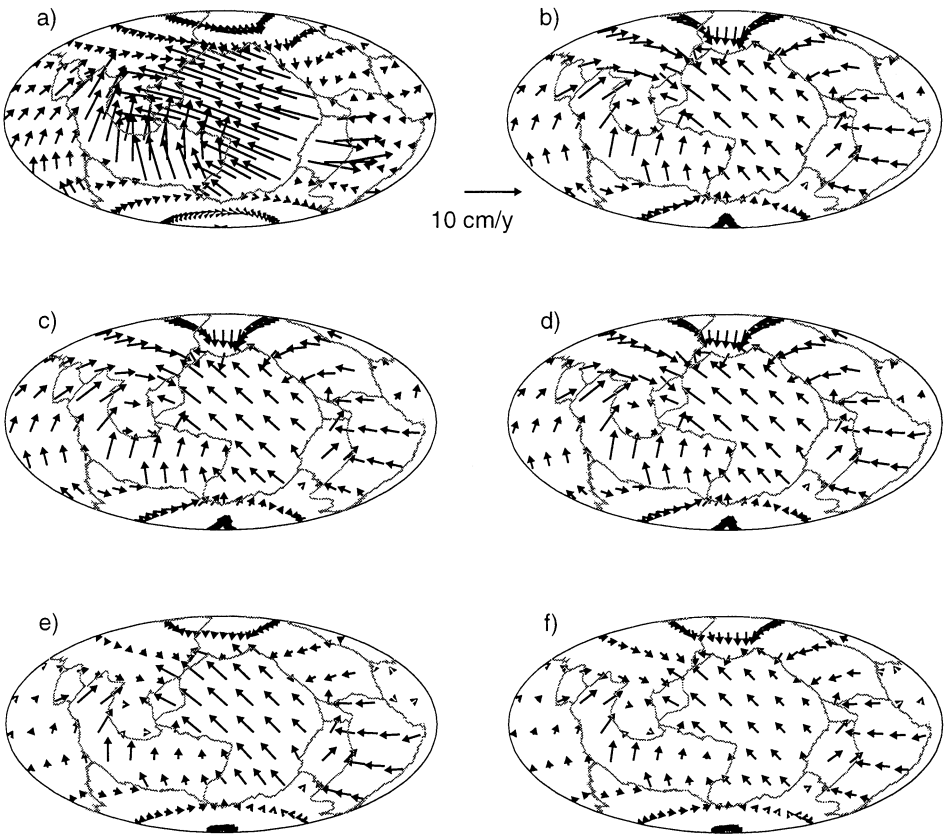

Figure 3. (a) The observed plate motion in a hot spot reference frame [*Gordon and Jurdy*, 1986] and model surface plate motion for cases (b) 1, (c) 2, (d) 3, (e) 4, and (f) 5. The upper mantle viscosity is assumed to be 10^{20} Pa s.

3. Results

This section presents five models that address the effects of more viscous continents (i.e., the ocean-continent contrast) and continental keels on the geoid and plate motion in the presence of weak plate margins.

3.1. Effects of the Ocean-Continent Contrast

Two cases are computed to investigate the effects of continents that are more viscous than oceanic lithosphere. Both cases (cases 1 and 2 in Table 1) include plate rheology with the same plate thickness. Case 1 assumes that continents have the same viscosity as oceanic plates. Case 1 is identical to a case of *Zhong and Davies* [1999] and is used for comparison. The geoid and plate motion from case 1 display the basic features of observations (Figures 2a, 2b, 3a, and 3b). *et al.*, 2000]. The geoid is computed from the dynamic topography and interior density anomalies with consideration of self-gravitation. The finite element grid has a horizontal resolution of ~100 km throughout the outer surface. In the radial direction, grid spacings for the lithosphere and the upper and lower mantle are about 20, 40, and 70 km, respectively.

In computing dimensional quantities the upper mantle viscosity is taken as 10^{20} Pa s, and the buoyancy is assumed to be half of that in the original slab model by *Ricard et al.* [1993]. For case 1 with the plate rheology, to reduce slab buoyancy by a factor of 2 leads to an optimal fit to the geoid. However, the variance reduction (~0.75) for case 1 is still less than that from the models with no plates by *Ricard et al.* [1993]. The reduced slab buoyancy leads to a smaller amplitude for dynamic topography, but the amplitude is still larger than inferred from the geological observations [*Ricard et al.*, 1993; *Gurnis*, 1990]. To reconcile model dynamic topography with the geological observations remains an important geodynamic problem [e.g., *Lithgow-Bertelloni and Richards*, 1998]. However, the current study will focus on the effects of continental structures on the geoid.

Plate motion resembles the observation for most oceanic plates (except the Nazca plate), but continental plates (e.g., the North American) move at comparable rates to oceanic plates, different from the observed (Figure 3b) [*Zhong and Davies*, 1999]. Similar plate motion was also found in previous models with a torque balance plate formulation [e.g., *Lithgow-Bertelloni and Richards*, 1998]. The surface motion in Figure 3b is with respect to a physically reasonable nonrotating mantle reference frame (Appendix A). As we shall see, surface motion may display net rotation with respect to this reference frame. However, for case 1 the surface motion contains negligibly small degree 1 toroidal field or net rotation (Figure 4a), even though the toroidal motion at other harmonic degrees (i.e., l>1) has significant power (Figure 4a) that is comparable with that of the poloidal motion (Figure 4b). The toroidal motion correlates well with the observation except at degree-1 (Figure 5c), while the minimum correlation of poloidal motion between case 1 and the observation is ~0.5 at degree 3 (Figure 5d).

Case 2 includes continents that are 10 times more viscous than oceanic lithosphere, and otherwise it is identical to case 1 (Table 1). Stiff continents in case 2 have only minor effects

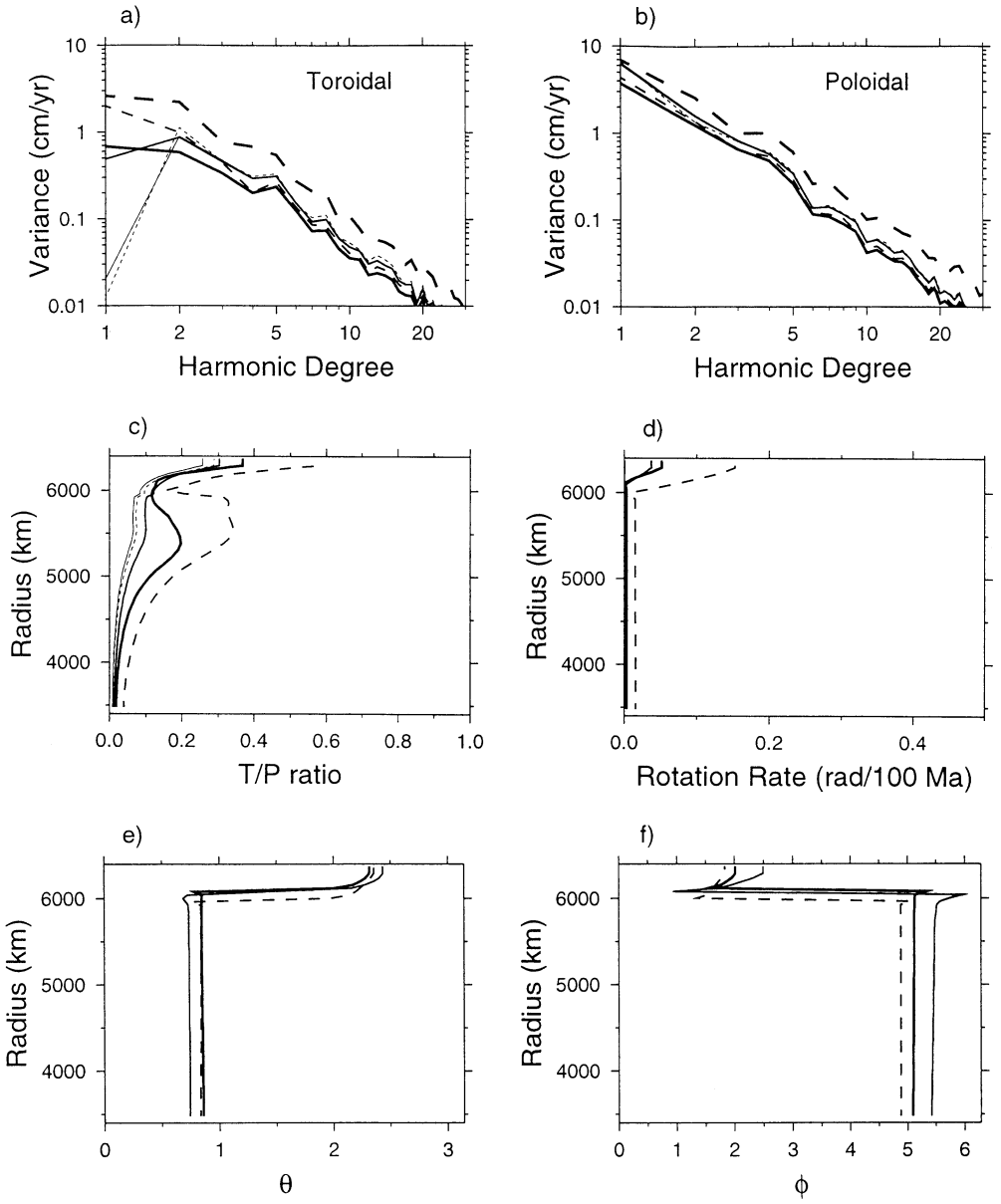

Figure 4. Degree variance for (a) toroidal and (b) poloidal plate motions. Radial dependence of (c) toroidal to poloidal ratio, (d) rotation rate, (e) coaltitude, and (f) longitude of rotation poles. In Figures 4a, 4b, and 4c, thin solid, thin dashed, intermediate solid, intermediate dashed, and thick solid lines are for cases 1, 2, 3, 4, and 5, respectively. In Figures 4a and 4b, thick dashed lines are for the observed plate motion [*Gordon and Jurdy*, 1986]. In Figures 4d, 4e and 4f, only results from cases 3, 4, and 5 are shown.

on the geoid (Figure 2c), as indicated by the similar correlation of the geoid to the observation for cases 1 and 2 (Figure 5a) and the high correlation between these two cases (Figure 5b). Stiff continents do not have significant effects on plate motion except for the slight increase in the African plate motion (Figure 3c). Compared with case 1, case 2 has identically small degree 1 toroidal motion (Figure 4a) and similar correlation of model plate motion to the observations (Figures 5c and 5d). Cases 1 and 2 also have a similar distribution of toroidal to poloidal ratio with depth. This ratio decreases rapidly with depth in the upper mantle (Figure 4c). This calculation indicates that the ocean-continent contrast in the presence of weak plate margins has negligible effects on the geoid and plate motion.

3.2. Effects of Continental Keels

We will now present three cases to examine the effects of continental keels. Cases 3 and 4 are identical to case 1 except that they include continental keels that extend to different depths (Figure 1b) (Table 1). Continental keels have the same viscosity as lithospheric viscosity. When continental keels only extend to a depth of 300 km (case 3), their influences on plate motion and the long-wavelength components of the geoid are insignificant (Figures 2d and 3d). However, continental keels may have significant amplifying effects on the regional geoid with the increased geoid high in the Siberian and African cratons and geoid low in the North American craton (Figure 2d). The geoid from case 3 is highly

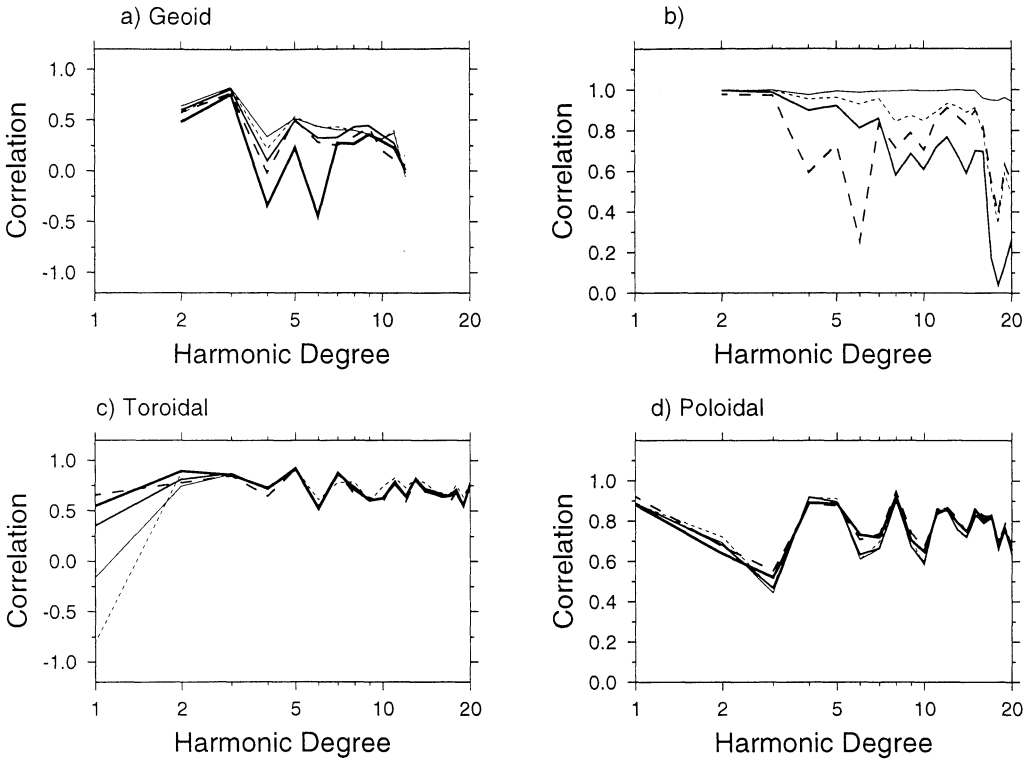

Figure 5. (a) Degree-to-degree correlation between the observed geoid and model geoid. (b) Degree-to-degree correlation of the geoid between case 1 and other cases. Degree-to-degree correlation of (c) toroidal and (d) poloidal plate motions between the observations and model predictions. In Figures 5a, 5c, and 5d, the line convention is identical to that for Figure 4a. In Figure 5b, thin solid, thin dashed, intermediate solid and intermediate dashed lines are for the correlation of case 1 to cases 2, 3, 4, and 5, respectively.

correlated with that from case 1 from degrees 2 to 15, but the correlation is reduced significantly at higher degrees (Figure 5b).

Continental keels in case 3 introduce important net rotation of lithosphere with respect to a nonrotating mantle reference frame (Figures 4a and 4d). The rate of net rotation is ~0.04 rad/100 Ma for lithosphere with the rotation pole centered at 50°S and 143°E. The rotation rate is much less than the observed 0.2 rad/100 Ma of *Gordon and Jurdy* [1986], and the location of rotation pole also differs significantly from the observed 40°S and 37°E. The inclusion of continental keels improves the correlation of degree 1 toroidal motion to the observation, while the correlation of toroidal motion at other degrees and of poloidal motion remains similar to that for case 1 (Figures 5c and 5d).

For case 3, the rate of net rotation decreases rapidly in the upper mantle before it reaches to a nonzero constant value at a depth of 300 km (Figure 4d). This indicates that the differential rotation occurs mainly between lithosphere and the rest of the mantle and that the transition happens over a 200-km-thick layer in the weak upper mantle. Since the mean rotation for the mantle and lithosphere must vanish by the definition for the nonrotating mantle reference frame (Appendix A), the rotation axis must change its orientation with depth (Figures 4e and 4f). The coordinates (i.e., colatitude θ and longitude ϕ) for the rotation pole are approximately constant within lithosphere and the lower mantle but vary with depth in the upper mantle (Figures 4e and 4f). Colatitude θ and longitude ϕ for rotation poles in the lower mantle differ from those in lithosphere by $\pi-\theta$ and π, respectively (Figures 4e and 4f), indicating a reversal of rotation vector from lithosphere to the lower mantle. This also indicates that the net rotation of lithosphere is primarily with respect to the high viscosity lower mantle.

Continental keels in case 4 extend to a depth of 410 km where transition zone viscosity is 30 times higher than that for the upper mantle (Table 1). Owing to the anchoring effects, continental keels exert greater effects on the geoid and plate motion (Figures 2e, 3e, and 5b). The local effects on the geoid become more evident with the affected regions that increase significantly (Figure 2e). As a result, the correlation of the geoid between cases 4 and 1 is <0.9 for degrees 6 and higher, although the correlation between these two cases remains high at long-wavelengths (degrees 2 to 5) (Figure 5b). However, the correlation to the observed geoid is significantly reduced at degree 4 as continental keels extend to a great depth (Figure 5a). Compared with case 1, plate motion for those continental plates with deep keels in case 4 is reduced (Figure 3e) owing to the strong coupling between the continental plates and relatively high-viscosity transition zone. However, the motion of North America is still too large compared with model motion for oceanic plates and with the observation, although a major continental keel is included there (Figure 1b). The motion for South America is not affected. This is because our models do not include continental keels for South America (Figure 1b).

The deeper continental keels in case 4 improve the correlation of degree 1 toroidal motion (to ~0.7 in Figure 5c) and produces lithospheric net rotation (i.e., ~0.16 rad/100 Ma rotation rate with 42°S and 103°E for the rotation pole) similar

to the observed (Figures 4a and 4d). By reducing continental motions, the deeper keels also reduce surface poloidal motion, particularly at degree 1 (Figure 4b). This leads to a larger ratio of toroidal to poloidal motion not only for lithosphere but also for the top 1200 km of the mantle (Figure 4c). However, this ratio (~0.58) at the surface is smaller than the observed.

The final case (case 5) with 300 km deep keels is identical to case 3 except that the viscosity in the upper mantle between 200 and 410 km depths is assumed to increase linearly with the depth by a factor of 10. Such an increase in the upper mantle viscosity is likely due to the pressure dependence of viscosity [e.g., *Karato and Wu*, 1993]. This calculation is used to assess whether shallow continental keels can effectively generate the observed lithospheric net rotation by coupling to higher-viscosity upper mantle. The increased upper mantle viscosity in case 5 reduces plate motion and its poloidal components (Figures 3f and 4b). However, because the reduction in plate motion is for both oceanic and continental plates, the lithospheric net rotation is similar to that from case 3 (Figures 4d, 4e and 4f). The geoid for case 5 (Figure 2f) differs significantly from that for case 1 at degree 4 and higher degrees (Figure 5b), suggesting a strong influence of radial viscosity on the geoid [*Hager and Richards*, 1989].

4. Discussions

4.1. Effects of Continental Structure on the Geoid

Our models show that when plate rheology (strong plate interiors and weak plate margins) is properly taken into account, the ocean-continent contrast and continental keels only have minor effects on long-wavelength (degrees 2 to 5) components of the geoid (Figures 2 and 5b). However, continental keels may have important effects at regional scales that are comparable with the keels (Figure 2). The regional effects on the geoid may have important implications to interpreting the observed gravity anomalies. For example, for continental keels extending to a depth of 300 km beneath North America, the regional negative geoid anomaly is nearly doubled in its magnitude, and such effects are stronger with deeper keels (Figures 2d and 2e). The large negative gravity anomaly in the Canadian shield may be caused by the combined effects of incomplete rebound since the last period of deglaciation [e.g., *Simons and Hager*, 1997] and mantle convection [*Pari and Peltier*, 1996]. Our models show that the high viscosity of continental keels is also capable of producing large negative gravity anomalies in this region.

Our models suggest that continental keels tend to amplify regional gravitational anomalies. While they result in more negative geoid in North America, continental keels induce larger positive geoid in Siberia and Africa (Figures 2d and 2e). This arises from a simple physics of stress coupling. If continental keels override negatively buoyant slabs, like those in North America, they enhance the coupling between the slabs and continents, thus increasing the depression of continents caused by the slabs. The mantle that is free from subducted slabs (e.g., below the Siberia and Africa for the slab model used in this study) may be viewed as relatively buoyant. Therefore the enhanced coupling due to the continental keels gives rise to more positive gravity anomalies (Figures 2d and 2e). Future studies on the dynamics and gravity of North America where slabs are clearly imaged in the middle of the mantle with seismic techniques [*van der Hilst et al.*, 1997] may pose important constraints on the mechanic structures of the North America continent.

The relatively small influence of continental structure on the long-wavelength geoid is consistent with the observation that the geoid does not correlate with distribution of continents. Weak plate margins play an important role in reducing the effects of continental structure on the long-wavelength geoid. When plates are effectively de-coupled from each other, strain is predominantly accommodated within the plate margins. This reduces the influences of continental structure on stress and flow fields with wavelengths that are larger than the scales of continents (Figures 3b, 3c and 5b).

4.2. Effects of Continental Structure on Plate Motion and Net Rotation of Lithosphere

In our models without continental keels, the Eurasian and North American plates move as rapidly as oceanic plates (Figures 3b and 3c for cases 1 and 2) [*Zhong and Davies*, 1999], similar to previous models with a different plate formulation [*Lithgow-Bertelloni and Richards*, 1998]. For these cases, while weak plate margins are effective in generating toroidal plate motion at degree 2 and higher degrees, net rotation between lithosphere and the mantle is negligible (Figure 4a). With the similar ocean and continent contrast to case 2, *Wen and Anderson* [1997] also found that no net rotation was generated. This indicates that lateral variations in viscosity at shallow depths (<100 km) including weak plate margins (i.e., case 1) and the ocean-continent contrast (i.e., case 2) may not necessarily produce net rotation of lithosphere. This result is different from that by *Ricard et al.* [1991], who found that significant net rotation could be produced with lateral variations in viscosity that are confined in a 100-km-thick shell overriding the mantle.

Our models show that continental keels or lithospheric thickness variations can generate net rotation of lithosphere with respect to the mantle. However, the net rotation is much smaller than the observed if the continental keels are confined in the upper mantle that is uniformly weak (case 3 in Figures 4a and 4d). This is because continental keels do not significantly increase the contact area of continental plates with the upper mantle to increase the coupling. Mantle flow in the upper mantle can easily divert away from the continental keels and therefore does not exert much influence on plate motion (Figures 3b and 3d). However, if continental keels extend to the high-viscosity transition zones, the increased coupling between continents and the underlying mantle can significantly slow down the continental motion (case 4 in Figure 3e) and introduce large net rotation of lithosphere (Figures 4a and 4d). Shallower continental keels may not provide the necessary coupling to generate lithospheric net rotation even if a reasonable viscosity increase with depth in the upper mantle due to the pressure dependence of viscosity is considered (Figures 3f, 4a and 4d for case 5).

Although continental keels that extend into the high-viscosity transition zone may reduce continental motion and produce large net rotation of lithosphere, it is unclear whether continental keels can be the primary cause for the observed slow continental motion and lithospheric net rotation for the following two reasons. (1) Seismic studies on the topography at the 410-km and 670-km discontinuities below the eastern North America suggest that continental keels may not extend to transition zones and that they do not perturb subcontinental

temperature [*Li et al.*, 1998]. (2) Studies on heat flow data from the Canadian shield including the largest Archean craton, the Superior province, and small-scale mantle convection indicate that the thickness of continental lithosphere for the Canadian shield is ~240-290 km and that sublithosphere temperature below the North American continental keel is similar to that at the same depth below ocean floors [*Jaupart et al.*, 1998]. If the derived thermochemical structure is representative, our models suggest that mantle temperature and pressure may not give rise to mantle viscosity below continental keels that would lead to sufficiently strong coupling between continents and their underlying mantle to cause the net rotation. The rapid motion of the Australian plate also suggests a relatively small role of continental keels on plate motion.

While a stronger coupling of continents to their underlying mantle through continental keels remains a plausible reason for producing slow continental motion and lithospheric net rotation, future studies may also need to examine other mechanisms. For example, preferential coupling of subducted slabs to oceanic plates may result in faster oceanic plate motion or asymmetric subduction. In addition, transform faults may differ from weak zones used in our models in the following way: weak zones are weak to both normal and tangential forces, but transform faults are strong to resist forces normal to the faults. More realistic treatment of plate margins may produce asymmetric subduction and pure strike-slip motion along transform faults [*Zhong and Gurnis*, 1996; *Conrad and Hager*, 1999]. This in combining with studies of regional gravity anomalies over continental cratons will eventually enable us to assess the relative role of continental keels and plate-plate coupling on the plate motion and net rotation of lithosphere.

5. Conclusions

Spherical shell models of mantle convection have been formulated to investigate the influences of the ocean-continent contrast and continental keels on plate motion and the geoid. The main conclusions are summarized as the follows:

1. The ocean-continent contrast and continental keels have minor effects on the long-wavelength geoid (for degrees 2-5) for plates that are effectively decoupled from each other. However, continental keels overriding subducted slabs can result in significant negative gravity anomaly at scales comparable with continental keels. This has important implications to interpreting the gravity anomalies in North America.

2. Dynamic models with weak zones bounding plates of the same thickness produce continental plate motion that is as large as oceanic plate motion and is too large compared with the observation. Continental keels as thick as 300 km cannot effectively reduce the continental plate motion to match with the observed if the sublithosphere viscosity below the keels is similar to that below oceanic plates. However, if no weak asthenosphere underlies the keels (for example, the keels extend into the high-viscosity transition zone), the keels may effectively couple to the deep mantle to produce the observed slow continental motion and lithospheric net rotation.

3. For models with weak zones bounding plates of the same thickness, neither weak plate margins nor the ocean-continent contrast can produce lithospheric net rotation, although weak plate margins produce toroidal motion at higher harmonics. Continental keels can effectively produce the net rotation. However, the net rotation is significantly smaller than the observed unless no weak asthenosphere exists below the keels (i.e., a stronger coupling between the upper mantle to continents than to oceanic plates). If the thermomechanic structure of North American continental upper mantle derived from seismic and heat flow studies is representative, our models suggest that mantle temperature and pressure may not yield mantle viscosity structure below the keels that would provide sufficient coupling between continents and their underlying mantle. Our study hints the necessity to include more realistic treatment of plate boundaries in future studies to assess possible effects of plate-plate coupling on plate motion.

Appendix A: Determination of Flow Velocity With Respect to a Nonrotating Mantle

For a buoyancy-driven flow the coupling between buoyancy force and lateral variations in viscosity introduces radial vorticity [*Ricard et al.*, 1991; *Forte and Peltier*, 1994]. On any spherical surface at a given radius the degree 1 component of radial vorticity represents a net rotation of this surface with respect to a reference frame in which the flow velocity is defined. A physically reasonable reference frame is a nonrotating mantle because the liquid outer core and atmosphere do not exert torque to the mantle [*Ricard et al.*, 1991]. However, such a nonrotating mantle reference frame may be difficult to be determined a prior, particularly in numerical models. This is partially because the dynamic equations do not constrain the mode of rigid body rotation. Depending on numerical methods, a reference frame can be set up either explicitly by pinning a grid point (e.g., for 2-D Cartesian or cylindrical finite element software ConMan with a direct solver [*King et al.*, 1990; *Zhong and Gurnis*, 1993]) or implicitly like those with iterative solvers. However, in such reference frames a rigid body rotation (or translation in a Cartesian geometry) may be introduced. Although the rigid body rotation does not affect the dynamics, it is often desired to remove the rigid body rotation. Here a procedure is presented to identify the rigid body rotation for an arbitrary velocity field in a spherical shell and to remove this rotation from the velocity field. The resulting velocity is thus referenced to a nonrotating mantle.

Define an arbitrary velocity field in a spherical shell as $\vec{V}(r,\theta,\phi)=[V_r,V_\theta,V_\phi]^T$ in a reference frame $\Re$ that may contain a rigid body rotation. We will determine the rigid body rotation vector $\vec{\omega}=\omega\vec{e}_p$, where ω is a rotation rate and $\vec{e}_p$ is a unit vector and can be expressed as

$$\vec{e}_p=[\sin\theta_p\cos\phi_p,\sin\theta_p\sin\phi_p,\cos\theta_p]^T, \qquad \text{(A1)}$$

where θ_p and ϕ_p are the colatitudinal and longitudinal coordinates for the rotation pole. We will first determine a rotation vector $\vec{\omega}_r=\omega_r\vec{e}_{pr}$ for spherical surface at each radius r, where $\vec{\omega}_r$ represents the net rotation of this surface with respect to $\Re$. Then the rigid body rotation vector $\vec{\omega}$ with respect to $\Re$ can be computed by averaging $\vec{\omega}_r$ over the entire spherical shell from the CMB at radius r_i to the surface at radius r_o:

$$\vec{\omega} = \frac{1}{(r_o - r_i)} \int_{r_i}^{r_o} \vec{\omega}_r dr. \quad \text{(A2)}$$

Now let us determine $\vec{\omega}_r$ for a spherical surface A_r with radius r. The radial vorticity on A_r can be computed with

$$\vec{e}_r \cdot \nabla \times \vec{V} = \Omega(\theta,\phi) = \frac{1}{r\sin\theta}\left[\frac{\partial(\sin\theta V_\phi)}{\partial\theta} - \frac{\partial V_\theta}{\partial\phi}\right]. \quad \text{(A3)}$$

It can be expressed in terms of spherical harmonics as

$$\Omega(\theta,\phi) = C_{10}\cos\theta + C_{11}\sin\theta\cos\phi + S_{11}\sin\theta\sin\phi + \sum_{l=2}^{l_{\max}}\sum_{m=0}^{l} D_{lm}Y_{lm}, \quad \text{(A4)}$$

where degree 1 terms are explicitly expressed with normalization coefficients for Y_{11} and Y_{10} that are incorporated into C_{10}, C_{11} and S_{11}.

Now we solve for the rotation vector $\vec{\omega}_r$ from the degree 1 terms in (A4). With coordinate transformation techniques, it can be shown that the azimuthal velocities (V_θ, V_ϕ) at any point (θ, ϕ) on A_r produced solely by rotation with angular velocity $\vec{\omega}_r$ can be expressed as

$$\begin{pmatrix} V_\theta \\ V_\phi \end{pmatrix} = \begin{pmatrix} r\omega_r \sin\theta_{pr}\sin(\phi_{pr} - \phi) \\ r\omega_r[\sin\theta\cos\theta_{pr} - \cos\theta\sin\theta_{pr}\cos(\phi_{pr} - \phi)] \end{pmatrix}, \quad \text{(A5)}$$

where θ_{pr} and ϕ_{pr} are the colatitudinal and longitudinal coordinates for the rotation pole. The resulting radial vorticity from velocities (A5) can be expressed as

$$\Omega_r = 2\omega_r(\cos\theta_{pr}\cos\theta + \sin\theta_{pr}\cos\phi_{pr}\sin\theta\cos\phi + \sin\theta_{pr}\sin\phi_{pr}\sin\theta\sin\phi) \quad \text{(A6)}$$

We can now solve for ω_r, θ_{pr} and ϕ_{pr} to obtain $\vec{\omega}_r$ by equating (A6) with the degree 1 terms in (A4):

$$\omega_r = \frac{1}{2}\sqrt{C_{10}^2 + C_{11}^2 + S_{10}^2}, \quad \text{(A7)}$$

$$\cos\theta_{pr} = \frac{C_{10}}{2\omega_r}, \quad \text{(A8)}$$

$$\tan\phi_{pr} = \frac{S_{11}}{C_{11}}. \quad \text{(A9)}$$

With (A2) the rigid body rotation vector $\vec{\omega}$ in the velocity field $\vec{V}(r,\theta,\phi)$ with respect to $\Re$ can be determined.

We now define a nonrotating mantle reference $\Re_{nr}$, and the velocity with respect to $\Re_{nr}$ can be obtained by subtracting velocity due to the rigid body rotation with angular velocity $\vec{\omega}$ from the original velocity $\vec{V}(r,\theta,\phi)$.

$$\begin{pmatrix} \tilde{V}_r \\ \tilde{V}_\theta \\ \tilde{V}_\phi \end{pmatrix} = \begin{pmatrix} V_r \\ V_\theta - r\omega\sin\theta_p\sin(\phi_p - \phi) \\ V_\phi - r\omega[\sin\theta\cos\theta_p - \cos\theta\sin\theta_p\cos(\phi_p - \phi)] \end{pmatrix}, \quad \text{(A10)}$$

where velocities with tilts are with respect to $\Re_{nr}$.

Acknowledgements. I would like to thank M. T. Zuber and M. Gurnis for their support and help, B. H. Hager for helpful discussion, Y. Ricard and C. Lithgow-Bertelloni for kindly providing me with their slab density models, S. Grand for providing his *S* wave tomography model, and U. Christensen, L. Fleitout, and an anonymous reviewer for constructive reviews. I also would like to thank K. C. Wong Educational Foundation of Hong Kong for a visiting fellowship.

References

Bercovici, D., A Source-sink model of the generation of plate tectonics from non-Newtonian mantle flow, *J. Geophys. Res., 100*, 2013-2030, 1995.

Bunge, H-P., M. A. Richards, and J. R. Baumgardner, Effect of depth-dependent viscosity on the planform of mantle convection, *Nature, 379*, 436-438, 1996.

Conrad, C. P., and B. H. Hager, Effects of plate bending and fault strength at subduction zones on plate dynamics, *J. Geophys. Res., 104*, 17551-17571, 1999.

Davies, G. F., Oceanic bathymetry and mantle convection, 1, Large-scale flow and hotspots, *J. Geophys. Res., 93*, 10467-10480, 1988.

Duncan, R. A., Hotspots in the southern oceans–An absolute frame of reference for motion of the Gondwana continents, *Tectonophysics, 74*, 29-42, 1981.

Forsyth, D. W., and S. Uyeda, On the relative importance of the driving forces of plate motion, *Geophys. J. R. Astron. Soc., 43*, 163-200, 1975.

Forte, A. M. and W. R. Peltier, The kinematics and dynamics of poloidal-toroidal coupling in mantle flow: The importance of surface plates and lateral viscosity variations, *Adv. in Geophys., 36*, 1-119, 1994.

Glatzmaier, G. A., G. Schubert, and D. Bercovici, Chaotic, subduction-like downflows in a spherical models of convection in the Earth's mantle, *Nature, 347*, 274-277, 1990.

Gordon, R. G., and D. M. Jurdy, Cenozoic global plate motions, *J. Geophys. Res., 91*, 12,389-12,406, 1986.

Grand, S. P., Mantle shear structure beneath the Americas and surrounding oceans, *J. Geophys. Res., 99*, 11,591-11,622, 1994.

Grand, S. P., R. D. van der Hilst, and S. Widiyantoro, Global seismic tomography: A snapshot of convection in the Earth, *GSA Today, 7*, 1-7, 1997.

Gurnis, M., A reassessment of the heat transport by variable viscosity convection with plates and lids, *Geophys. Res. Lett., 16*, 179-182, 1989.

Gurnis, M., Bounds on global dynamic topography from Phanerozoic flooding of continental plateforms, *Nature, 344*, 754-756, 1990.

Gurnis, M., and T. H. Torsvik, Rapid drift of large continents during the late precambrian and Paleozoic paleomagnetic constraints and dynamic models, *Geology, 22*, 1023-1026, 1994.

Hager, B. H., Subducted slabs and the geoid: constraints on mantle rheology and flow, *J. Geophys. Res., 89*, 6003-6015, 1984.

Hager, B. H., and R. J. O'Connell, Subduction zone dip angles and flow driven by plate motion, *Tectonophysics, 50*, 111-133, 1978.

Hager, B. H., and M. A. Richards, Long-wavelength variations in Earth's geoid: Physical models and dynamical implications, *Philos. Trans. R. Soc. London, Ser. A, 328*, 309-327, 1989.

Jaupart, C., J. C. Mareschal, L. Guillou-Frottier, and A. Davaille, Heat flow and thickness of the lithosphere in the Canadian shield, *J. Geophys. Res., 103*, 15,269-15,286, 1998.

Karato, S., and P. Wu, Rheology of the upper mantle: A synthesis, *Science, 260*, 771-778, 1993.

King, S. D., and B. H. Hager, The Relationship between plate velocity and trench viscosity in Newtonian and power-law subduction calculations, *Geophys. R. Lett., 17*, 2409-2412, 1990.

King, S. D., A. Raefsky, and B. H. Hager, ConMan: Vectorizing a finite element code for incompressible two-dimensional convection in the Earth's mantle, *Phys. Earth Planet. Inter., 59*, 195-207, 1990.

Li, A, K. M. Fisher, M. E. Wysession, and T. J. Clarke, Mantle discontinuities and temperature under the North American continental keel, *Nature, 395*, 160-163, 1998.

Li, X-D., and B. A. Romanowicz, Global mantle shear velocity model developed using nonlinear asymptotic coupling theory, *J. Geophys. Res., 101*, 22,245-22,272, 1996.

Lithgow-Bertelloni, C., and M. A. Richards, The dynamics of Cenozoic and Mesozoic plate motions, *Rev. Geophys., 36*, 27-78, 1998.

Manga, M., and R. J. O'Connell, The tectosphere and postglacial rebound, *Geophys. Res. Lett., 22*, 1949-1952, 1995.

Masters, G., S. Johnson, G. Laske, H. Bolton, A Shear-Velocity Model of the Mantle, *Philos. Trans. R. Soc. London, Ser. A, 354*, 1385-1410, 1996.

Minster, J. B. and T. H. Jordan, Present-day plate motions, *J. Geophys. Res.*, *83*, 5331-5354, 1978.

Molnar, P., and J. Stock, Relative motions of hotspots in the Pacific, Atlantic, and Indian Ocean since late Cretaceous time, *Nature*, *230*, 42-43, 1987.

Moreši, L., and M. Gurnis, Constraints on the lateral strength of slabs from three-dimensional dynamic flow models, *Earth Planet. Sci. Lett.*, *138*, 15-28, 1996.

Moresi, L., and V. S. Solomatov, Mantle convection with a brittle lithosphere-Thoughts on the global tectonic styles of the Earth and Venues, *Geophys. J. Int.*, *133*, 669-682, 1998.

Morgan, W. J., Hotspot tracks and the early rifting of the Atlantic, *Tectonophysics*, *94*, 123-139, 1983.

O'Connell, R. J., C. W. Gable, and B. H. Hager, Toroidal-poloidal partitioning of lithospheric plate motion, in *Glacial Isostasy, Sea Level and Mantle Rheology*, edited by R. Sabadini and K. Lambeck, pp. 513-535, Kluwer Acad. Norwell, Mass., 1991.

Pari, G., and W. R. Peltier, The free-air gravity constraint on subcontinental mantle dynamics, *J. Geophys. Res.*, *101*, 28,105-28,132, 1996.

Pollack, H. N., Cratonization and thermal evolution of the mantle, *Earth Planet. Sci. Lett.*, *80*, 175-182, 1986.

Ratcliff, J. T., G. Schubert, and A. Zebib, Steady tetrahedral and cubic patterns of spherical-shell convection with temperature-dependent viscosity, *J. Geophys. Res.*, *101*, 25,473-25,484, 1996.

Ricard, Y., C. Doglioni, and R. Sabadini, Differential rotation between lithosphere and mantle: A consequence of lateral mantle viscosity variations, *J. Geophys. Res.*, *96*, 8407-8415, 1991.

Ricard, Y., M. A. Richards, C. Lithgow-Bertelloni, and Y. L. Stunff, A geodynamic model of mantle density heterogeneity, *J. Geophys. Res.*, *98*, 21,895-21,909, 1993.

Ritzwoller, M. H., and E. M. Lavely, Three-dimensional seismic models of the Earth's mantle, *Rev. of Geophys.*, *33*, 1-66, 1995.

Shapiro, S. S., B. H. Hager, and T. H. Jordan, Stability and dynamics of the continental tectosphere, *LITHOS*, *48*, 115-133, 1999.

Simons, M., and B. H. Hager, Localization of the gravity field and the signature of glacial rebound, *Nature*, *390*, 500-504, 1997.

Sleep, N. H., Hotspots and mantle plumes: Some phenomenology, *J. Geophys. Res.*, *95*, 6715-6736, 1990.

Su, W.-J., R. L. Woodward, and A. M. Dziewonski, Degree 12 model of shear velocity heterogeneity in the mantle, *J. Geophys. Res.*, **99**, 6945-6980, 1994.

Turcotte, D. L., and G. Schubert *Geodynamics* , John Wiley, New York, 1982.

van der Hilst, R. D., S. Widiyantoro, and E. R. Engdahl, Evidence for deep mantle circulation from global tomography, *Nature*, *386*, 578-584, 1997.

Van der Voo, R., W. Spakman, and H. Bijwaard, Mesozoic subducted slabs under Siberia, *Nature*, *397*, 246-249, 1999.

Wen, L., and D. L. Anderson, Present-day plate motion constraint on mantle rheology and convection, *J. Geophys. Res.*, *102*, 24,639-24,653, 1997.

Woodhouse, J. H., and A. M. Dziewonski, Mapping of the upper mantle three dimensional modelling of Earth structure by inversion of seismic waveforms, *J. Geophys. Res.*, *89*, 5953-5986, 1984.

Zhang, S., and U. R. Christensen, Some effects of lateral viscosity variations on geoid and surface velocities induced by density anomalies in the mantle, *Geophys. J. Int.*, *114*, 531-547, 1993.

Zhong, S., and G. F. Davies, Effects of plate and slab viscosities on the geoid, *Earth Planet. Sci. Lett.*, *170*, 487-496, 1999.

Zhong, S., and M. Gurnis, Dynamic feedback between an non-subducting raft and thermal convection, *J. Geophys. Res.*, *98*, 12,219-12,232, 1993.

Zhong, S., and M. Gurnis, Interaction of weak faults and non-Newtonian rheology produces plate tectonics in a 3D model of mantle flow, *Nature*, *383*, 245-247. 1996.

Zhong, S., M. Gurnis, and L. Moresi, The role of faults, nonlinear rheology, and viscosity structure in generating plates from instantaneous mantle flow models, *J. Geophys. Res.*, *103*, 15,255-15,268, 1998.

Zhong, S., M. T. Zuber, L. Moresi, and M. Gurnis, Role of temperature-dependent viscosity and surface plates in spherical shell models of mantle convection, *J. Geophys. Res.*, *105*, 11,063-11,082, 2000.

S. Zhong, Department of Physics, University of Colorado, Boulder, CO 80309-0390. (szhong@anquetil.colorado.edu)

(Received February 4, 2000; revised September 18, 2000;
accepted September 28, 2000.)